Author Manuscript

Author Manuscript

Author Manuscript

Author Manuscript

HHS Public Access

Author manuscript

Chemosphere. Author manuscript; available in PMC 2018 November 28.

Published in final edited form as:

Chemosphere. 2013 November ; 93(9): 1997–2003. doi:10.1016/j.chemosphere.2013.07.019.

Fractal structures of single-walled carbon nanotubes in biologically relevant conditions: Role of chirality vs. media conditions

Iftheker A. Khan[a], **Nirupam Aich**[a], **A.R.M. Nabiul Afrooz**[a], **Joseph R.V. Flora**[a], **P. Ariette Schierz**[b], **P. Lee Ferguson**[c], **Tara Sabo-Attwood**[d], and **Navid B. Saleh**[a,*]

[a]Department of Civil and Environmental Engineering, University of South Carolina, Columbia, SC 29208, USA

[b]Department of Civil, Architectural, and Environmental Engineering, University of Texas, Austin, TX 78712, USA

[c]Department of Civil and Environmental Engineering, Duke University, Durham, NC 27708, USA

[d]Department of Environmental and Global Health, University of Florida, Gainesville, FL 32610, USA

Abstract

Aggregate structure of covalently functionalized chiral specific semiconducting single-walled carbon nanotubes (SWNTs) was systematically studied employing static light scattering (SLS). Fractal dimensions (D_f) of two specific chirality SWNTs—SG65 and SG76 with (6, 5) and (7, 6) chiral enrichments—were measured under four biological exposure media conditions, namely: Dulbecco's Modified Eagle Medium (DMEM), Minimum Essential Medium (MEM), Roswell Park Memorial Institute (RPMI) 1640 medium, and 0.9% saline solution. The SWNTs exhibited chiral dependence on D_f with SG65 showing more fractal or loosely bound aggregate structures, i.e., lower D_f values (range of 2.24 ± 0.03 to 2.64 ± 0.05), compared to the SG76 sample (range of 2.58 ± 0.13 to 2.90 ± 0.08). All the D_f values reported are highly reproducible, measured from multiple SLS runs and estimated with 'random block-effects' statistical analysis that yielded all p values to be <0.001. The key mechanism for such difference in D_f between the SWNT samples was identified as the difference in van der Waals (VDW) interaction energies of these samples, where higher VDW of SG76 resulted in tighter packing density. Effect of medium type showed lower sensitivity; however, presence of di-valent cations (Ca^{2+}) in DMEM and MEM media resulted in relatively loose or more fractal aggregates. Moreover, presence of fetal bovine serum (FBS) and bovine serum albumin (BSA), used to mimic the *in vitro* cell culture condition, reduced the D_f values, i.e., created more fractal structures. Steric hindrance to aggregation was identified as the key mechanism for creating the fractal structures. Also, increase in FBS concentration from 1% to 10% resulted in increasingly lower D_f values.

*Corresponding author. Tel.: +1 (803) 777 2288. salehn@engr.sc.edu (N.B. Saleh).

Appendix A. Supplementary material

Supplementary data associated with this article can be found, in the online version, at http://dx.doi.org/10.1016/j.chemosphere.2013.07.019.

Author Manuscript Author Manuscript Author Manuscript Author Manuscript

GRAPHICAL ABSTRACT

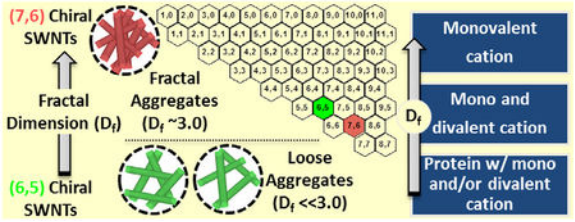

Keywords

Fractal dimension; Aggregation; Single-walled carbon nanotubes; Static light scattering; Chirality

1. Introduction

Single-walled carbon nanotubes (SWNTs), tubular structures of sp^3 hybridized carbon atoms, provide unique electrical, mechanical, and optical properties (Iijima and Ichihashi, 1993; Forro et al. 2000; Baughman et al., 2002; Xia et al., 2003). Variations of tube diameter and atomic arrangement of carbon, together known as chirality, introduce added advantages to these helicoids and thus widen the application premise to drug delivery, therapeutics, and electronics (Thostenson et al., 2001; Bachilo et al., 2002; Minot et al., 2003; Chen et al., 2010). The growing market transfer of such SWNT-laden applications has contributed to increased market share, projected to be $1.5 billion by 2015 (Mehta, 2010; NRC, 2012). Such commercialization has generated added concerns for this emerging nanomaterial and necessitates reliable studies for fate, exposure, and risk implications (Oberdorster et al., 2005; Klaine et al., 2008). Aggregation propensity of nanomaterials, particularly that of SWNTs, is well known in the literature to have profound implications for fate, transport, and biological exposure (Jaisi and Elimelech, 2009; Kang et al., 2009; Saleh et al., 2010). Particles at the nanoscale exhibit unique properties that allow surface energies to dominate their behavior. The interplay between inherent van der Waals forces and other specific and non-specific surface interactions—e.g., electrostatic, hydrophobic, and ligand-receptor interactions, entropic forces, etc.—determine particle stability and organization at this scale (Elimelech et al., 1995; Espinasse et al., 2007). Aggregate structural organization can play a key role in nanomaterial aqueous fate as well as biological responses. However, the state-of-the-art literature is limited to aggregate size evaluation with little or no consideration for the aggregate structures of the SWNTs.

Interfacial interactions of nanoscale materials get altered with the change in surface chemistry and physical attributes and are well known to have significant impact on their aggregation behavior. SWNTs, all carbon tubules, are also known to have unique aggregation behavior as a function of the aforementioned parameters (Zhang et al., 2009; Saleh et al., 2010; Forney et al., 2011; Bouchard et al., 2012; Khan et al., 2013). To-date, the aggregation behavior of SWNTs is systematically studied as a function of covalent and non-covalent surface functionality and in presence of a range of background chemistry, i.e., inorganic salts and various bio-macromolecules (Saleh et al., 2010; Bouchard et al., 2012; Khan et al., 2013). The key findings in aggregation studies of SWNTs primarily determine

Author Manuscript Author Manuscript Author Manuscript Author Manuscript

their aggregation state at various regimes with an effort to delineate mechanisms in response to the surrounding chemistry. The physicochemical differences thus contributing to SWNT cluster size are proved to have notable impact on their environmental fate and biological interaction. The tubular physical features, highly bundled aggregation state, as well as ability to adsorb hydrophobic biomacromolecules are known to have influenced biological responses of SWNTs (Yang et al., 2010; Philbrook et al., 2011; Pasquini et al., 2012). It is also important to note that differences in physicochemical attributes not only influence aggregation dynamics but also will influence particle–particle interaction and thus packing density of aggregated particles. Recently, covalent functionalization of SWNTs with varied aggregate structure showed fractal structure dependent cytotoxicity (Pasquini et al., 2012); which generates an urgent need for systematic evaluation of aggregate structure in biological exposure conditions.

Structural morphology of aggregates has classically been analyzed in colloidal literature by measuring fractal dimension (D_f) (Weitz et al., 1985; Sorensen, 2001; Bushell et al., 2002). Analytical methods are established employing static light scattering (SLS) or low angle X-ray scattering (LAXS) on polystyrene latex, silica, and other uniform colloids (Guo et al., 1990; Odriozola et al., 2001; Bushell et al., 2002; Martinez-Pedrero et al., 2005). The foundation of such analytical techniques is based on the principle of angle-dependent scattering of electromagnetic waves (both visible and X-ray waves); where the angular dependence is proved to be a function of aggregate packing density (Asnaghi et al., 1995; Sorensen, 2001; Bushell et al., 2002). Though the fundamentals of D_f determination have strong foundation on physical theories, yet have limited applications in nanoscale materials reflected through only a handful of studies reporting D_f values (Chen et al., 2004; Sun et al., 2004; Kim et al., 2008; Lebedev et al., 2010; Kumar et al., 2012; Pasquini et al., 2012; Meng et al., 2013). Though angle-dependent detection of scattered visible waves (for SLS) is proved to be the most promising technique for D_f measurement of nanomaterials, significant challenges remain in obtaining reliable structural information (Chen et al., 2004; Pasquini et al., 2012; Meng et al., 2013). SWNTs, possessing a complex bundled and clustered structure, are uniquely different compared to classical colloidal matrices; thus present key challenges of reproducibility for the measured D_f, using conventional SLS studies and data analysis. The studies to-date, presenting D_f of SWNTs, fail to report confidence in their measured values by accounting for run-specific uncertainty and thus allow a sustained data gap for reliable D_f prediction. Additionally, physical parameters, e.g., chirality, though influence optical, electronic, mechanical or chemical properties of SWNTs, the impact of such parameters on aggregate structure is yet to be determined.

The objective of this study is to systematically address this data gap of reliable determination of D_f, for chiral-specific SWNTs in different biologically relevant exposure conditions. The chiral-specific SWNTs are covalently functionalized to achieve near-equal surface functionality. Four cell culture media, i.e., Dulbecco's Modified Eagle Medium (DMEM), Minimum Essential Medium (MEM), Roswell Park Memorial Institute (RPMI) Medium 1640, and 0.9% Saline solution are considered as control media. Two different serum supplements, i.e., fetal bovine serum (FBS) and bovine serum albumin (BSA) were also added into the control media to mimic the *in vitro* cell culture condition. The scattered light intensity data was collected as a function of scattering angle and classical SLS

Author Manuscript Author Manuscript Author Manuscript Author Manuscript

technique coupled with systematic statistical analysis is employed to evaluate SWNT fractal dimension with (6, 5) and (7, 6) SWNT chiralities. Detailed physicochemical and electrokinetic characterizations are performed using transmission electron microscopy (TEM), Raman spectroscopy, and electrophoretic mobility (EPM) measurements.

2. Materials and methods

2.1. Chiral SWNTs

CoMoCAT SWNTs were procured from SouthWest NanoTechnologies Inc. (SWeNT, Norman, OK, USA). Two different types of semiconducting SWNTs were tested in this study: SG65 (lot No. 000–0031) and SG76 (lot No. 0020) tubes with predominantly (6, 5) and (7, 6) chiral enrichment (Khan et al., 2013). The chirality distribution of SWNTs was confirmed by NIR spectroscopy. Detailed chirality map and its NIR characterization data is reported in the earlier study (Khan et al., 2013). A chirality map showing (6, 5) and (7, 6) chiral indices is shown in Fig. S1.

2.2. Media

Biological osmotic fluid 0.9% saline solution (Cat. No. 101448–952, VWR) and three cell culture media, namely: DMEM (Cat. No. 11885–084, invitrogen), MEM (Cat. No. 11575–032, invitrogen), and RPMI 1640 medium (Cat. No. 11835–030, invitrogen) were used as stock media. The standard bovine serum albumin (BSA) solution at 2 mg mL^{-1} concentration (Cat. No. 23210, Fisher Sci.) and heat inactivated fetal bovine serum (FBS) at similar concentration (Cat. No. 16140–063, Invitrogen) were used to mimic the serum supplement conditions for *in vitro* cell culture systems.

2.3. Optimized Covalent Functionalization

The SWNTs were covalently functionalized following a two-step process. 5 mg of SWNTs were bath sonicated (Branson 1510) in 2.5 mL of 6 M HNO_3 to remove metal impurities for a duration of 1 h (Li et al., 2004). Later, the purified SWNTs were bath sonicated with 2.5 mL concentrated H_2SO_4/HNO_3 mixture (3:1, 98% and 70% strength, respectively) for 4 h (Liu et al., 1998; Li et al., 2004). After each step, SWNT suspension was filtered through 200 nm polypropylene (GHP) membranes (Pall Life Science, Port Washington, NY) and rinsed with Milli-Q water until the pH of the filtrate reached ~6.5. The filtered sample was then dried for 3 h at 60°C and kept in a silica gel chamber for 3 d. The conditions, i.e., sonication intensity, duration, oxidant composition, etc., were optimized using previously established sonication technique (Khan et al., 2013) to achieve near-equal surface functionalization as verified by parallel characterization with XPS, Raman spectroscopy, and electrophoretic mobility measurements (EPM). Careful covalent functionalization of SG65 and SG76 yielded similar length tubes.

2.4. Characterization of SWNTs

Transmission electron microscopic characterizations of the single walled carbon nanotubes were performed to investigate their structural and bundling morphology in pristine, functionalized, and in-media forms. Details of TEM method are described elsewhere (Saleh et al., 2008, 2010). In short, 5 mL of ~15 mg L^{-1} SWNT solution was prepared in ethyl

Author Manuscript Author Manuscript Author Manuscript Author Manuscript

alcohol (JT Baker, ACS Grade) and sonicated for 10 min using a sonic dismembrator (S-4000, Misonix). Suspensions were then placed in a bath sonicator for 15 min prior to imaging and a drop of each suspension was placed on a 200-mesh copper TEM grid coated with carbon formvar (Ted Pella Inc.). Excess solvent was removed by wicking with filter paper and the grid was allowed to dry in a hot plate at 75°C for 15 min. Images were collected using an H-9500 (300 kV) TEM (Hitachi High Technologies America, Inc, CA) with 0.18 nm resolution. Malvern Zetasizer (ZEN 3660) system was used to measure the EPM of the different chiral samples in various media conditions using established protocol described elsewhere (Saleh et al., 2008, 2010; Afrooz et al., 2013). In short, diluted stock solution at ~1 mg L^{-1} concentration was maintained. Medium solutions were added immediately prior to the EPM measurements and all measurements were conducted with at least three replicate samples to ensure reproducibility.

2.5. Fractal Dimension Measurement with SLS

Aggregate structure information was determined through fractal dimensions, D_f measurements. ALV/CGS-3 precision goniometer system (ALV-GmbH, Langen, Germany) was used in angle-dependent static light scattering (SLS) mode, which employs a 22 mW He–Ne laser (632.8 nm wavelength) equipped with ALV/LSE-5004 Light Scattering Digital Correlator (ALV-GmbH, Langen, Germany). For these experiments, 2 mL of solution of nanotubes in media were added to disposable borosilicate glass vials (Fisher Scientific, Pittsburg, PA). These vials were soaked in 2% cleaning solution (Extran MA01, EMD Chemicals, Gibbstown, NJ), and thoroughly rinsed with deionized water, and finally, oven dried (Fisher Scientific, Pittsburg, PA) under dust free conditions.

The scattered light intensity "I" was detected by a photon counting module operating at 1.2 amperes and 5 volts made by Perkin Elmer (Dumberry, Canada) and the data was collected as a function of scattering angle that varied from 12° to 150° in 0.5° increment. To ensure that the suspensions maintain quasi-equilibrium in terms of their colloidal stability, each measurement was started 60 min after the addition of the SWNTs to media (Kim and Berg, 2000; Bushell et al., 2002). This time period was set by performing time resolved dynamic light scattering experiments, where stable aggregate size achieving time guided such selection. The scattered light intensity (I) is related to the absolute value of scattering vector (q), which is a function of the angle at which the intensity was collected at; Eq. (1) describes the relation between I, q and D_f.

$$I = q^{-D_f} \quad (1)$$

Scattering vector q was determined using Eq. (2) that correlates it with medium refractive index (n), laser wavelength (λ) and scattering angle (θ). Linear fractal regime of scattering was identified and fitted with a straight line to determine D_f.

Author Manuscript Author Manuscript Author Manuscript Author Manuscript

$$q = \frac{4\pi n}{\lambda}\sin\left(\frac{\theta}{2}\right) \quad (2)$$

Usually, the reported D_f in the literature does not incorporate run specific uncertainty; i.e., each angle-dependent run results in uncertainty in linear fit to acquire a D_f value, which cannot be averaged to obtain a statistically reliable parameter. This paper addresses run-specific uncertainty of I vs. q dataset utilizing a regression model with 'random block-effects'. Statistical Analytical System (SAS) software package (Version 9.3, SAS Institute Inc.) was employed, where 'proc mixed' process—that is based on maximum likelihood principle—with a random block variable captured run-specific uncertainty. All the D_f values reported in this study had undergone the statistical optimization. It is to be noted that D_f values for all conditions tested in this study showed high likelihood shown by the strong confidence in the determined p-value <0.001. The software code used for the statistical analysis is included in Fig. S2.

3. Results and discussion

3.1. SWNT physicochemical characterization

The SWNT characterization with TEM and EPM measurements contributed to the understanding of their morphological characteristics and electrokinetic behavior in different media conditions. Representative TEM micrographs of pristine and covalent functionalized SWNTs are presented in Fig. S3. Bundled and relatively long SWNT tubes are shown in Fig. S3(a and b), while substantial shortening and debundling of tubes are evident from Fig. S3(c and d). Both the SG65 and SG76 chiral SWNTs showed similar debundling and shortening that are similar to earlier reported work from the authors (Khan et al., 2013). Also, such changes in SWNT morphology upon covalent functionalization are consistently observed elsewhere in the literature (Sun et al., 2002; Saleh et al., 2010).

Electrokinetic characterization of SWNTs shows similar negative surface potential for SG65 and SG76 at different media conditions (Fig. 1). For SG65 and SG76, the EPM values were determined to be $-(1.34 \pm 0.33)\times10^{-8}$ and $-(1.81 \pm 0.36) \times 10^{-8}$ for DMEM, $-(1.36 \pm 0.4) \times 10^{-8}$ and $-(1.69 \pm 0.31) \times 10^{-8}$for MEM, $-(0.93 \pm 0.3) \times 10^{-8}$ and $-(1.31 \pm 0.35) \times 10^{-8}$ for RPMI, and $-(2.14 \pm 0.46) \times 10^{-8}$ and $-(2.31 \pm 0.40) \times 10^{-8}$ m^2 V^{-1} s^{-1} for saline condition. The results show that chirality plays relatively insignificant role in electrokinetic properties of the SWNTs, while covalently functionalized with a strong oxidant. The similar values and relatively low magnitude of EPM are likely caused by substantial electrostatic screening due to the presence of high concentration of cations in biological media and saline solutions. Similar EPM values were reported earlier for higher salt conditions. For similar acid functionalization EPM of $-(1.22 \pm 0.20) \times 10^{-8}$ and $-(0.92 \pm 0.20) \times 10^{-8}$ m^2 V^{-1} s^{-1} for SG65 and $-(0.99 \pm 0.08) \times 10^{-8}$ and $-(0.72 \pm 0.02) \times 10^{-8}$ m^2 V^{-1} s^{-1} was reported for 100 and 200 mM NaCl conditions, respectively (Khan et al., 2013). Mechanochemically stabilized SWNTs showed EPM values of -0.46×10^{-8} m^2 V^{-1} s^{-1} at 55 mM NaCl (Saleh et al., 2010). Whereas, non-covalently functionalized, i.e., SDBS modified SWNTs, also

Author Manuscript Author Manuscript Author Manuscript Author Manuscript

showed relatively low values of ζ-potential; i.e., −18 and −15 mV, for 140 and 200 mM NaCl, respectively (Ju et al., 2012).

3.2. Fractal structure of SWNTS in different media

The scattering intensity data are plotted with respect to the angle-dependent scattering vector in Fig. 2 for both SG65 and SG76 SWNTs at all media condition. The fractal structure of SWNTs as determined by SLS is presented in Fig. 2(c). Overall, the D_f showed small difference between different background media conditions, however, demonstrate a strong chirality dependence. The SG65 SWNTs consistently displayed lower D_f values ranging from 2.24 ± 0.03 to 2.64 ± 0.05, compared to SG76 SWNTs with range of 2.58 ± 0.13 to 2.90 ± 0.08. The lowest D_f was observed for DMEM and MEM media where as the higher values were yielded from using RPMI and saline background conditions. It is to be noted that the relative value of D_f signifies aggregate structure conformation; i.e., closer the D_f value is to the value of 3.0, more compact is the aggregate structure, whereas a D_f value of near 1.0 value signifies looser aggregate structure (Mukhopadhyay et al., 2012; Schaeublin et al., 2012). The relatively higher D_f values for saline and RPMI media are likely due to the sole presence of mono-valent cations, compared to mono- and di-valent cation presence in case of DMEM and MEM media conditions (Weitz et al., 1985; Kim and Berg, 2000; Odriozola et al., 2001; Meng et al., 2013).

It is also to be noted that for all the media conditions, presence of high amount of salt—i.e., >130 mM Na^+ for all media and 1–2 mM Ca^{2+} for DMEM and MEM—has presented favorable aggregation regime for the SWNTs with a nearly complete electrostatic screening. Thus, the key interaction forces dominating in this region is most likely the tube-tube interaction forces and van der Waals attractive interaction. It is well known that higher electro-static screening, results in ‘sticky colloids’, which typically yields loosely bound aggregate structure; i.e., low D_f values (Weitz et al., 1985; Kim and Berg, 2000; Odriozola et al., 2001; Meng et al., 2013). The SG65 tubes with relatively lower van der Waals interaction thus displays relatively low D_f values for DMEM and MEM media conditions.

On the other hand, a substantially high van der Waals interaction that exists between SG76 tubes (Khan et al., 2013) has likely dominated the aggregation process and thus resulted in relatively higher D_f values; i.e., more compact aggregate structures. It is noteworthy that di-valent electrolyte played a significant role in formation of the aggregation structures. Absence of di-valent Ca^{2+} for both RPMI and saline conditions has caused the SWNTs to pack more closely and yield higher D_f values, compared to the DMEM and MEM media conditions with 1–2 mM Ca^{2+} cations. A slightly higher degree of electrostatic screening has most likely caused the SWNTs to be ‘stickier’ in presence of di-valent cations those results in such differences.

The fractal structure and relatively compactness of SWNT aggregates are further observed through TEM imaging in presence of background media conditions. Fig. 3 shows differences in aggregate compactness, primarily caused through the tube–tube interaction differences between SG65 and SG76. Relatively lower degree of tube–tube interaction for SG65 resulted in loosely bound SWNTs (Fig. 3a and c) compared to closely packed SG76 (Fig. 3b and d), likely caused from higher van der Waals interaction between these tubes. The TEM

Author Manuscript Author Manuscript Author Manuscript Author Manuscript

images are a visual proof of the D_f measurements, showing relative differences in compactness.

3.3. Role of biomolecules on fractal structure

Nanomaterial exposure media often contains biomolecules such as globular protein BSA (Elgrabli et al., 2007; Qiu et al., 2010; Saleh et al., 2010) and a more complex enzymetic and protein mixture of FBS (Hu et al., 2011) at different concentrations. Understanding the aggregate structure in presence of these essential biomolecular additives will likely provide further insight onto SWNT aggregation and its impact to biological responses (Pasquini et al., 2012). Fig. 4 shows the role of BSA on D_f. Addition of BSA shows a decrease in D_f for both SG65 and SG76 from 2.61 ± 0.13 to 2.52 ± 0.14 and 2.89 ± 0.08 to 2.56 ± 0.06, respectively. These results indicate that presence of globular BSA proteins has likely caused a more loosely packed aggregate structure for both SWNTs and essentially diminished the role of chirality on packing density. The likely mechanism for such decrease in D_f can be examined studying the interplay between electrokinetic and physical contribution of BSA molecules on aggregation.

Fig. S4a shows EPM values of both SG65 and SG76, where both the tubes show lower electrostatic potential in presence of BSA. It indicates that a slight decrease in EPM might have been caused by attachment of BSA molecules onto the SWNT surfaces and thereby causing a subsequent shielding of electrokinetic potential. Thus the lower electrokinetic potential contributed to increased ‘stickiness’ of the tubes which has likely contributed toward lower D_f values. Furthermore, the globular structure of BSA proteins has also likely contributed to steric hindrances to attachment, and thereby caused a looser aggregate structure for both SG65 and SG76. Such evidences of steric interaction from BSA molecules were previously reported for SWNT aggregation (Saleh et al., 2010).

A more complex biomolecule mixture FBS is also typically added to exposure media during in vitro studies. The FBS mixture essentially contains enzymes as well as the BSA proteins, which have high likelihood of causing substantial differences in aggregate structure formation. Results presented in Fig. 5 shows consistent decrease in D_f for the increased addition of FBS (from 1% to 10%)

for SG65 for all media conditions. For SG76, the trend was similar except for RPMI medium. It is to be noted that increased amount of FBS did not reduce D_f for SG76 in case of RPMI. We believe that the RPMI media lacks in di-valent cation presence, which reduced the electrostatic screening and allowed for enhanced dominance of van der Waals interaction between SG76 tubes and resulted in compact aggregate structure. It is to be again noted that higher diameter SG76 possess higher van der Waals interaction forces when compared to SG65, as reported earlier (Khan et al., 2013).

Further evidences of loosening of SWNT aggregate structures are observed through TEM imaging as presented in Fig. S5. In presence of 10% FBS, both SG65 and SG76 showed looser packing of aggregates; when compared to the media only cases. It is also evident that in absence of FBS, the packing density is observed to be higher for SG76 compared to SG65, as consistently observed in earlier TEMs. The role of FBS on aggregate structure

Author Manuscript Author Manuscript Author Manuscript Author Manuscript

formation can also be evaluated using eletrokinetic properties and physical contribution from biomolecular interaction. EPM results in presence of FBS show a consistent decrease with the increase in FBS concentration for both SG65 and SG76 (Fig. S4b and c). The trend is similar to the decrease in D_f values as observed in Fig. 5. Similar to the BSA molecules, a more complex mixture of biomolecules FBS has likely caused sorption to SWNT surfaces and provided with strong shielding of electrokinetic interaction. The higher the FBS concentration, the higher is the FBS amount onto SWNTs and more is the shielding. Moreover, increased amount of FBS also provided with higher steric hindrances between SWNTs, which also contributed toward lowering of D_f values for both SG65 and SG76 SWNTs.

4. Conclusions

Fractal dimension can serve as a key parameter influencing biological interaction and environmental fate of SWNTs. During biological exposure, particularly for *in vitro* studies, the SWNTs undergoes interfacial interaction in response to the surrounding media conditions prior to interacting with the substrates; that usually is placed at the bottom of the exposure cells. Thus, aggregation of SWNTs as a result of electrostatic screening alongside with unique fractal structure formation will influence the true exposure of the SWNT aggregates to the cellular entities. Lower the D_f, looser is the packing density, higher will be the fluid drag onto the SWNT clusters. Thus true exposure of low D_f SWNT samples will be a lot lower compared to that of more compact high D_f aggregates. Similarly, fractal structure will also influence the fate of SWNTs in environmental systems. Fractal SWNTs will undergo similar fluid drag in surface water conditions that will likely result in a more persistent SWNT transport in such systems, compared to higher D_f more compact SWNT structures—which will likely settle faster due to increased gravity and lower drag. It is important to note that nanoparticulate recognition by cellular matrices depend on particle type and structure and thereby can be influenced by aggregate structure variation of the SWNTs. Moreover, SWNT transport in groundwater systems will also be influenced by aggregate structure. The lower the D_f, the more likely will be the propensity of the SWNT clusters to undergo physical filtration. Thus SWNTs with low D_f in saline environment will likely undergo higher degree of filtration. Therefore, aggregate structure information is an important physicochemical parameter that needs to be determined for a complete and reliable understanding of nano-bio interaction and nanomaterial fate in the environment.

Supplementary Material

Refer to Web version on PubMed Central for supplementary material.

Acknowledgements

Funding was provided by the National Science Foundation (CBET 0933484). We are grateful to Dr. Haijun Qian of Clemson Microscopy Center for his kind assistance in TEM imaging.

Author Manuscript Author Manuscript Author Manuscript Author Manuscript

References

Afrooz ARMN, Sivalapalan ST, Murphy CJ, Hussain SM, Schlager JJ, Saleh NB, 2013 Spheres vs. rods: the shape of gold nanoparticles influences aggregation and deposition behavior. Chemosphere 91, 93–98. [PubMed: 23246723]

Asnaghi D, Carpineti M, Giglio M, Vailati A, 1995 Light-scattering-studies of aggregation phenomena. Phys. A 213, 148–158.

Bachilo SM, Strano MS, Kittrell C, Hauge RH, Smalley RE, Weisman RB, 2002 Structure-assigned optical spectra of single-walled carbon nanotubes. Science 298, 2361–2366. [PubMed: 12459549]

Baughman RH, Zakhidov AA, de Heer WA, 2002 Carbon nanotubes – the route toward applications. Science 297, 787–792. [PubMed: 12161643]

Bouchard D, Zhang W, Powell T, Rattanaudompol US, 2012 Aggregation kinetics and transport of single-walled carbon nanotubes at low surfactant concentrations. Environ. Sci. Technol 46, 4458–4465. [PubMed: 22443301]

Bushell GC, Yan YD, Woodfield D, Raper J, Amal R, 2002 On techniques for the measurement of the mass fractal dimension of aggregates. Adv. Colloid Interface Sci 95, 1–50. [PubMed: 11843188]

Chen Q, Saltiel C, Manickavasagam S, Schadler LS, Siegel RW, Yang HC, 2004 Aggregation behavior of single-walled carbon nanotubes in dilute aqueous suspension. J. Colloid Interface Sci 280, 91–97. [PubMed: 15476778]

Chen KJ, Nair N, Strano MS, Braatz RD, 2010 Identification of chirality-dependent adsorption kinetics in single-walled carbon nanotube reaction networks. J. Comput. Theor. Nanosci 7, 2581–2585.

Elgrabli D, Abella-Gallart S, Aguerre-Chariol O, Robidel F, Rogerieux F, Boczkowski J, Lacroix G, 2007 Effect of BSA on carbon nanotube dispersion for in vivo and in vitro studies. Nanotoxicology 1, 266–278.

Elimelech M, Gregory J, Jia X, Williams RA, 1995 Particle Deposition and Aggregation: Measurement, Modelling and Simulation. Elsevier.

Espinasse B, Hotze EM, Weisner MR, 2007 Transport and retention of colloidal aggregates of C60 in porous media: effect of organic macromolecules, ionic composition, and preparation method. Environ. Sci. Technol 41, 7396–7402. [PubMed: 18044517]

Forney MW, Anderson JS, Ameen AL, Poler JC, 2011 Aggregation kinetics of single-walled carbon nanotubes in nonaqueous solvents: critical coagulation concentrations and transient dispersion stability. J. Phys. Chem C 115, 23267–23272.

Forro L, Salvetat J-P, Bonard, Bacsa R, Thomson NH, Garaj S, Thien-Nga L, Gaal R, Kulik A, Ruzicka B, Degiorgi L, Bachtold A, Schönenberger C, Pekker S, Hernadi K, 2000 Electronic and mechanical properties of carbon nanotubes In: Tománek DERJ (Ed.), Science and Application of Nanotubes. Kluwer Academic/Plenum Publishers, New York.

Guo XH, Zhao NM, Chen SH, Teixeira J, 1990 Small-angle neutron-scattering study of the structure of protein detergent complexes. Biopolymers 29, 335–346. [PubMed: 2331502]

Hu WB, Peng C, Lv M, Li XM, Zhang YJ, Chen N, Fan CH, Huang Q, 2011 Protein corona-mediated mitigation of cytotoxicity of graphene oxide. ACS Nano 5, 3693–3700. [PubMed: 21500856]

Iijima S, Ichihashi T, 1993 Single-shell carbon nanotubes of 1-nm diameter. Nature 363, 603–605.

Jaisi DP, Elimelech M, 2009 Single-walled carbon nanotubes exhibit limited transport in soil columns. Environ. Sci. Technol 43, 9161–9166. [PubMed: 20000506]

Ju L, Zhang W, Wang X, Hu J, Zhang Y, 2012 Aggregation kinetics of SDBS-dispersed carbon nanotubes in different aqueous suspensions. Colloids Surf., A 409, 159–166.

Kang S, Mauter MS, Elimelech M, 2009 Microbial cytotoxicity of carbon-based nanomaterials: implications for river water and wastewater effluent. Environ. Sci. Technol 43, 2648–2653. [PubMed: 19452930]

Khan IA, Afrooz ARMN, Flora JRV, Schierz PA, Ferguson PL, Sabo-Attwood T, Saleh NB, 2013 Chirality affects aggregation kinetics of single-walled carbon nanotubes. Environ. Sci. Technol 47, 1844–1852. [PubMed: 23343128]

Author Manuscript Author Manuscript Author Manuscript Author Manuscript

Kim AY, Berg JC, 2000 Fractal aggregation: scaling of fractal dimension with stability ratio. Langmuir 16, 2101–2104.

Kim T, Lee CH, Joo SW, Lee K, 2008 Kinetics of gold nanoparticle aggregation: experiments and modeling. J. Colloid Interface Sci 318, 238–243. [PubMed: 18022182]

Klaine SJ, Alvarez PJJ, Batley GE, Fernandes TF, Handy RD, Lyon DY, Mahendra S, McLaughlin MJ, Lead JR, 2008 Nanomaterials in the environment: behavior, fate, bioavailability, and effects. Environ. Toxicol. Chem 27, 1825–1851. [PubMed: 19086204]

Kumar S, Aswal VK, Kohlbrecher J, 2012 Size-dependent interaction of silica nanoparticles with different surfactants in aqueous solution. Langmuir: ACS J. Surf. Colloids 28, 9288–9297.

Lebedev VT, Grushko YS, Orlova DN, Kim AF, Kozlov VS, Sedov VP, Kolesnik SG, Shamanin VV, Melenevskaya EY, 2010 Aggregation in hydroxylated endohedral fullerene solutions. Fuller. Nanotub. Carbon Nanostruct 18, 422–426.

Li Y, Zhang X, Luo Z, Huang W, Cheng J, Luo Z, Li T, Liu F, Xu G, Ke X, Li L, Geise HJ, 2004 Purification of CVD synthesized single-wall carbon nanotubes by different acid oxidation treatments. Nanotechnology 15, 1645–1649.

Liu J, Rinzler AG, Dai H, Hafner JH, Bradley RK, Boul PJ, Lu A, Iverson T, Shelimov K, Huffman CB, Rodriguez-Macias F, Shon Y-S, Lee TR, Colbert DT, Smalley RE, 1998 Fullerene pipes. Science 280, 1253–1256. [PubMed: 9596576]

Martinez-Pedrero F, Tirado-Miranda M, Schmitt A, Callejas-Fernandez J, 2005 Aggregation of magnetic polystyrene particles: a light scattering study. Colloid Surf. A – Physicochem. Eng. Asp 270, 317–322.

Mehta M, 2010 2009 NCMS Study of Nanotechnology in the U.S. Manufacturing Industry. National Center for Manufacturing Sciences, Ann Arbor, MI.

Meng Z, Hashmi SM, Elimelech M, 2013 Aggregation rate and fractal dimension of fullerene nanoparticles via simultaneous multiangle static and dynamic light scattering measurement. J. Colloid Interface Sci 392, 27–33. [PubMed: 23211871]

Minot ED, Yaish Y, Sazonova V, Park JY, Brink M, McEuen PL, 2003 Tuning carbon nanotube band gaps with strain. Phys. Rev. Lett, 90.

Mukhopadhyay A, Grabinski C, Afrooz ARMN, Saleh N, Hussain S, 2012 Effect of gold nanosphere surface chemistry on protein adsorption and cell uptake in vitro. Appl. Biochem. Biotechnol 167, 327–337. [PubMed: 22547299]

NRC, 2012 A Research Strategy for Environmental, Health, and Safety Aspects of Engineered Nanomaterial. National Research Council of The National Academies, Washington, DC.

Oberdorster G, Oberdorster E, Oberdorster J, 2005 Nanotoxicology: an emerging discipline evolving from studies of ultrafine particles. Environ. Health Perspect 113, 823–839. [PubMed: 16002369]

Odriozola G, Tirado-Miranda M, Schmitt A, Lopez FM, Callejas-Fernandez J, Martinez-Garcia R, Hidalgo-Alvarez R, 2001 A light scattering study of the transition region between diffusion- and reaction-limited cluster aggregation. J. Colloid Interface Sci 240, 90–96. [PubMed: 11446790]

Pasquini LM, Hashmi SM, Sommer TJ, Elimelech M, Zimmerman JB, 2012 Impact of surface functionalization on bacterial cytotoxicity of single-walled carbon nanotubes. Environ. Sci. Technol 46, 6297–6305. [PubMed: 22515158]

Philbrook NA, Walker VK, Afrooz A, Saleh NB, Winn LM, 2011 Investigating the effects of functionalized carbon nanotubes on reproduction and development in Drosophila melanogaster and CD-1 mice. Reprod. Toxicol 32, 442–448. [PubMed: 21963887]

Qiu Y, Liu Y, Wang LM, Xu LG, Bai R, Ji YL, Wu XC, Zhao YL, Li YF, Chen CY, 2010 Surface chemistry and aspect ratio mediated cellular uptake of Au nanorods. Biomaterials 31, 7606–7619. [PubMed: 20656344]

Saleh NB, Pfefferle LD, Elimelech M, 2008 Aggregation kinetics of multiwalled carbon nanotubes in aquatic systems: measurements and environmental implications. Environ. Sci. Technol 42, 7963–7969. [PubMed: 19031888]

Saleh NB, Pfefferle LD, Elimelech M, 2010 Influence of biomacromolecules and humic acid on the aggregation kinetics of single-walled carbon nanotubes. Environ. Sci. Technol 44, 2412–2418. [PubMed: 20184360]

Author Manuscript Author Manuscript Author Manuscript Author Manuscript

Schaeublin NM, Braydich-Stolle LK, Maurer EI, Park K, MacCuspie RI, Afrooz ARMN, Vaia RA, Saleh NB, Hussain SM, 2012 Does shape matter? bioeffects of gold nanomaterials in a human skin cell model. Langmuir 28, 3248–3258. [PubMed: 22242624]

Sorensen CM, 2001 Light scattering by fractal aggregates: a review. Aerosol Sci. Technol 35, 648–687.

Sun Y-P, Fu K, Lin Y, Huang W, 2002 Functionalized carbon nanotubes: properties and applications. Acc. Chem. Res 35, 1096–1104. [PubMed: 12484798]

Sun CH, Li F, Ying Z, Liu C, Cheng HM, 2004 Surface fractal dimension of single-walled carbon nanotubes. Phys. Rev. B, 69.

Thostenson ET, Ren ZF, Chou TW, 2001 Advances in the science and technology of carbon nanotubes and their composites: a review. Compos. Sci. Technol 61, 1899–1912.

Weitz DA, Huang JS, Lin MY, Sung J, 1985 Limits of the fractal dimension for irreversible kinetic aggregation of gold colloids. Phys. Rev. Lett 54, 1416–1419. [PubMed: 10031026]

Xia YN, Yang PD, Sun YG, Wu YY, Mayers B, Gates B, Yin YD, Kim F, Yan YQ, 2003 One-dimensional nanostructures: synthesis, characterization, and applications. Adv. Mater 15, 353–389.

Yang CN, Mamouni J, Tang YA, Yang LJ, 2010 Antimicrobial activity of single-walled carbon nanotubes: length effect. Langmuir 26, 16013–16019. [PubMed: 20849142]

Zhang SJ, Shao T, Bekaroglu SSK, Karanfil T, 2009 The impacts of aggregation and surface chemistry of carbon nanotubes on the adsorption of synthetic organic compounds. Environ. Sci. Technol 43, 5719–5725. [PubMed: 19731668]

Author Manuscript Author Manuscript Author Manuscript Author Manuscript

HIGHLIGHTS

- SWNTs form chirality dependent fractal aggregates.
- The (6, 5) enrichment is likely to attain loose structures compared to (7, 6) ones.
- Higher van der Waals energy is responsible for tighter aggregates in (7, 6).
- Presence of di-valent Ca^{2+} and FBS/BSA lowers the D_f values.
- Steric hindrance likely caused the loose aggregate structures.

Author Manuscript Author Manuscript Author Manuscript Author Manuscript

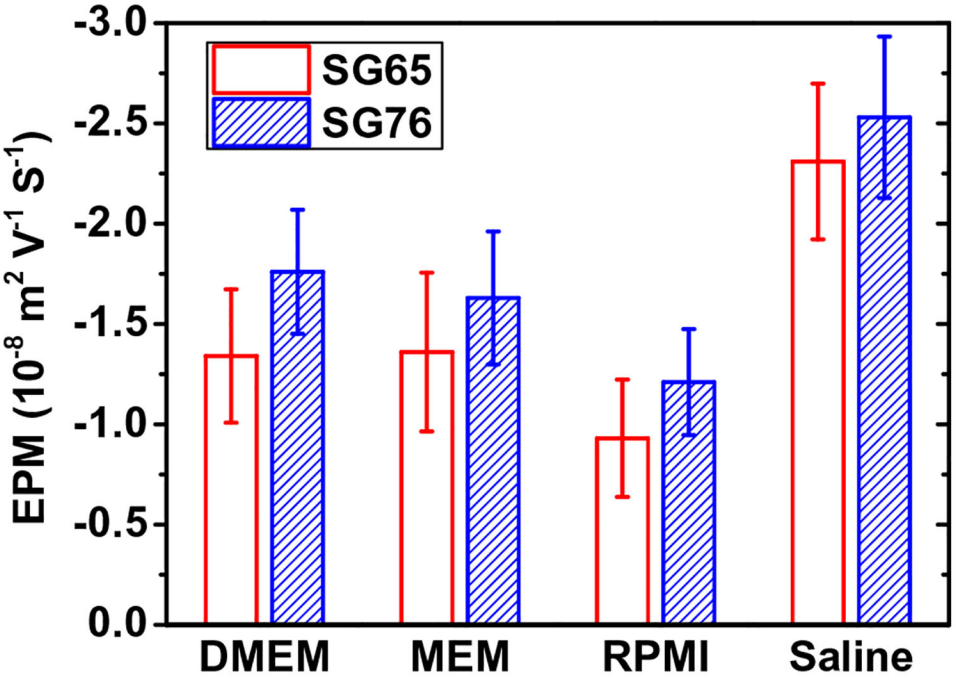

Fig. 1.

Electrophoretic mobility (EPM) of SWNTs under four different media i.e., DMEM, MEM, and RPMI and 0.9% Saline solution. At least three separate experiments were performed for each condition and data presented here are mean of three independent experiments with one standard deviation. Measurements were carried out at a pH of ~6.5 and a temperature of 20°C.

Author Manuscript Author Manuscript Author Manuscript Author Manuscript

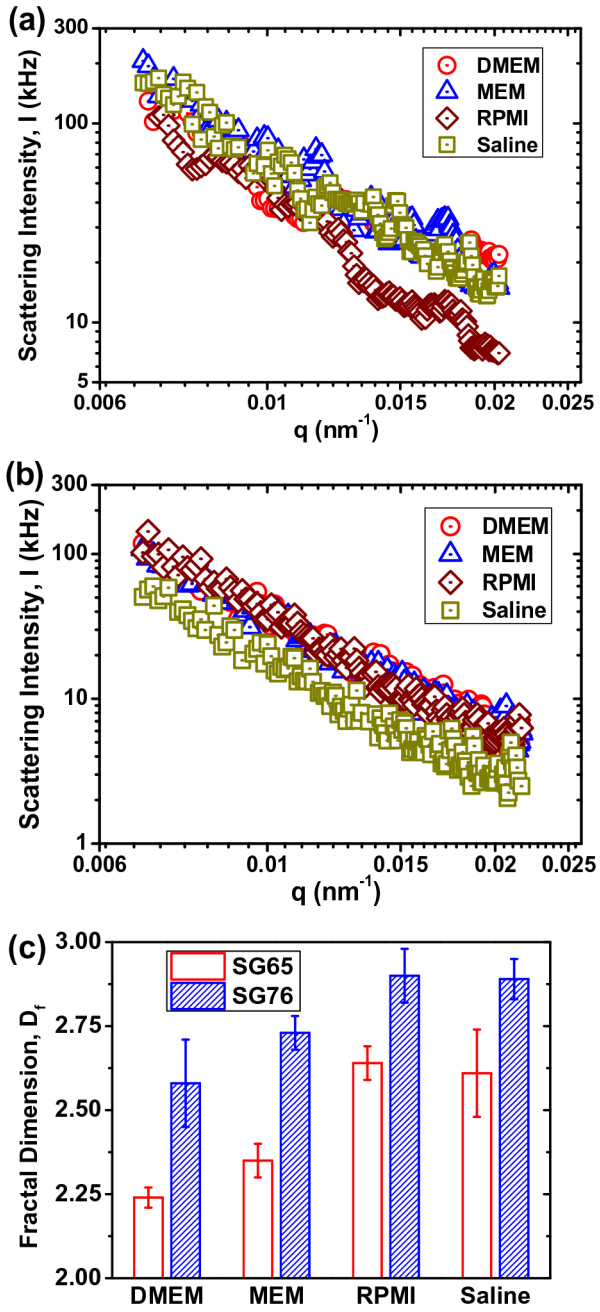

Fig. 2.

Scattering intensity (*I*) data with change in scattering vector (*q*) under four different media conditions: DMEM, MEM, RPMI and 0.9% Saline solution for (a) SG65 and (b) SG76 SWNTs. All the Static light scattering (SLS) measurements were carried out at least thrice at a pH of ~6.5 and at 20°C. (c) Fractal dimension (D_f) of SG65 and SG76 SWNTs, estimated from (a) and (b), respectively. All the reported D_f values showed p value <0.001.

Author Manuscript Author Manuscript Author Manuscript Author Manuscript

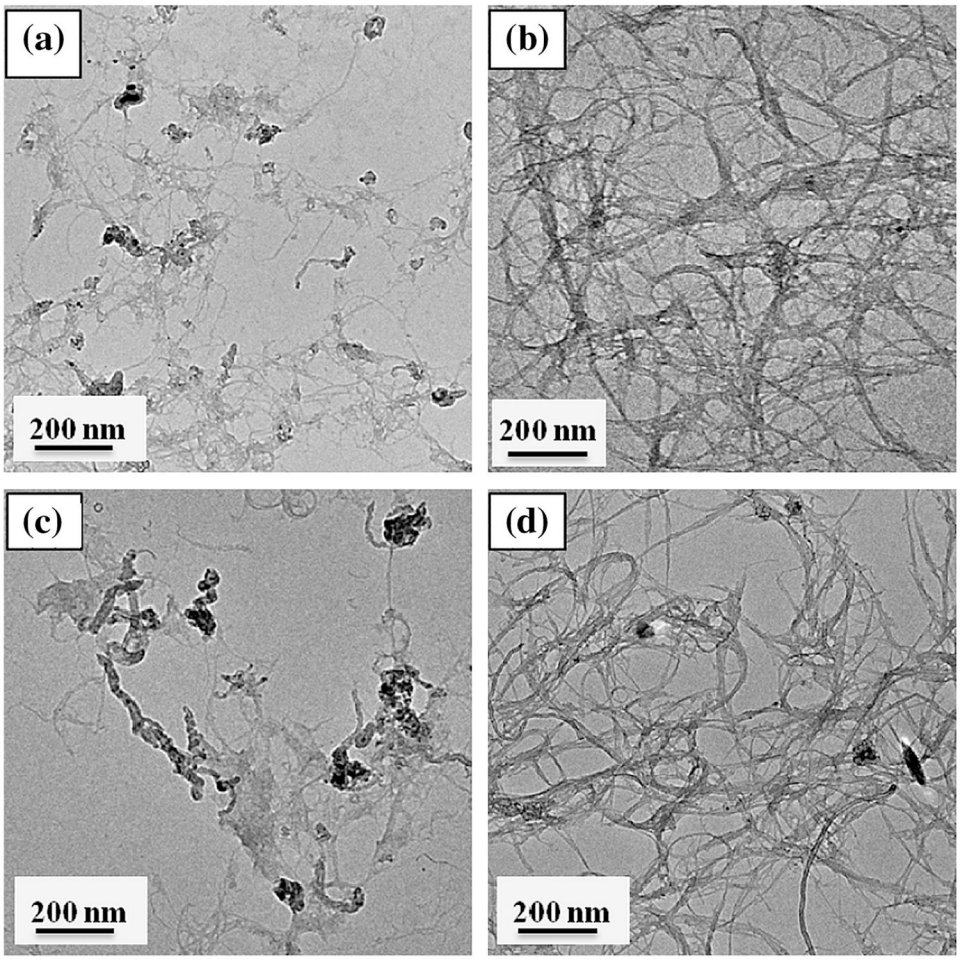

Fig. 3.

TEM micrographs of representative SWNTs: (a) SG65 w/RPMI (D_f = 2.64 ± 0.05), (b) SG76 w/RPMI (D_f = 2.90 ± 0.08), (c) SG65 w/Saline (D_f = 2.61 ± 0.13), and (d) SG76 w/Saline (D_f = 2.89 ± 0.06).

Author Manuscript Author Manuscript Author Manuscript Author Manuscript

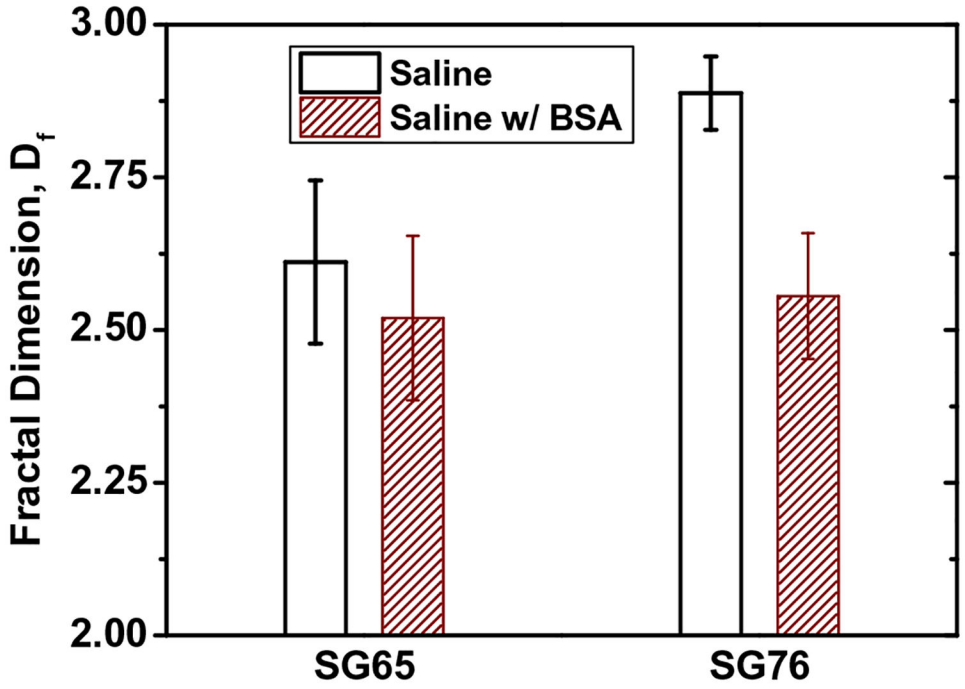

Fig. 4.

Effect of BSA on fractal dimension (D_f) of SG65 and SG76 SWNTs in control media (i.e. 0.9% Saline solution). All the reported D_f values showed p value <0.001 for at least triplicate runs.

Author Manuscript Author Manuscript Author Manuscript Author Manuscript

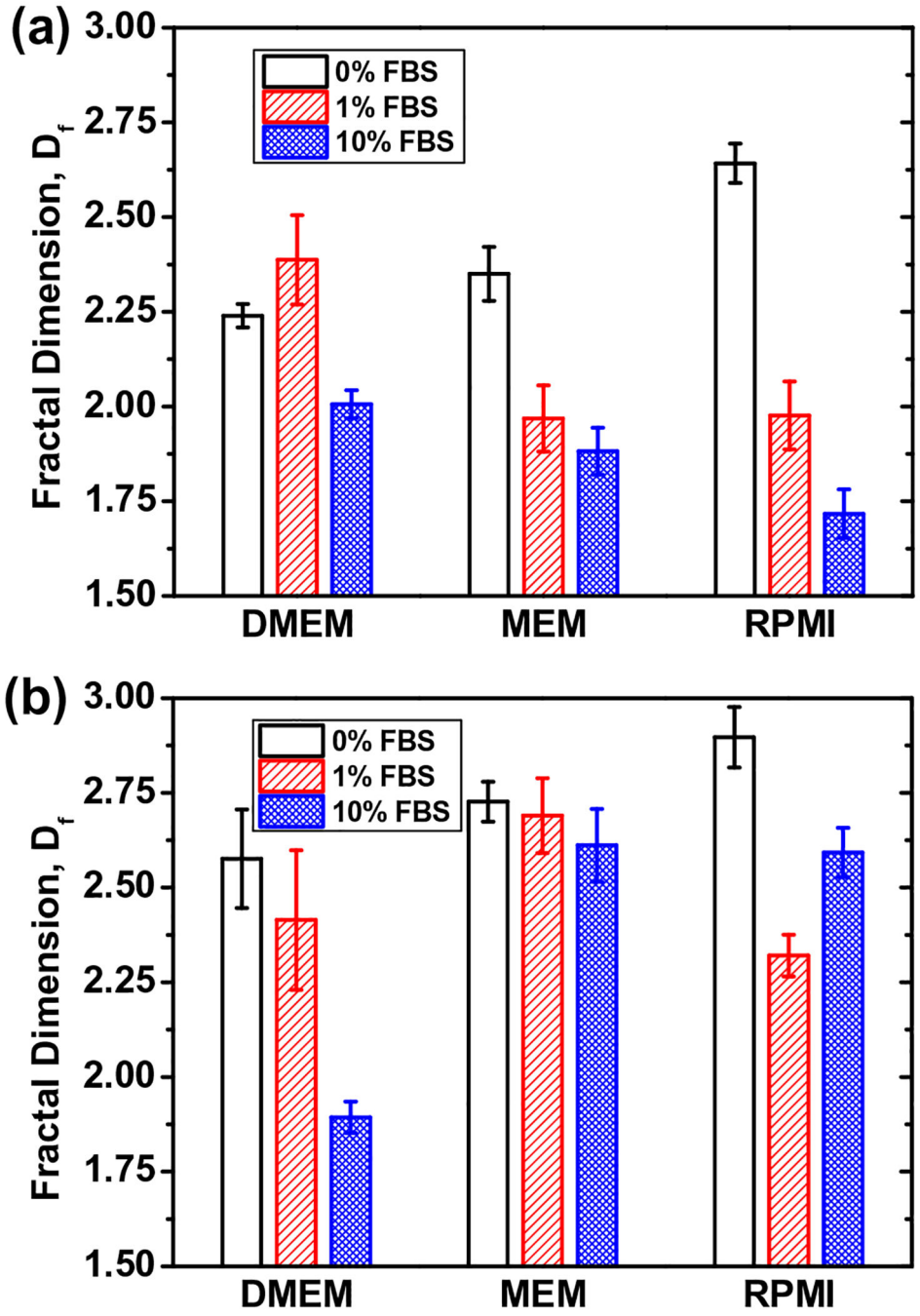

Fig. 5.

Fractal dimension (D_f) values of (a) SG65 and (b) SG76 SWNTs in presence of 0%, 1%, and 10% FBS added to DMEM, MEM, and RPMI 1640 medium. All reported D_f values showed p value <0.001 for triplicate runs.